

THERMAL STABILIZATION OF A THERMIONIC
DIODE COLLECTOR

Robert Edwin Schantz

NAVAL POSTGRADUATE SCHOOL

Monterey, California



THESIS

THERMAL STABILIZATION
of
A THERMIONIC DIODE COLLECTOR

by

Robert Edwin Schantz

Thesis Advisor

M. Wilcox

December 1971

Approved for public release; distribution unlimited.

Thermal Stabilization
of
A Thermionic Diode Collector

by

Robert Edwin Schantz
Lieutenant, United States Navy
B.S., The Pennsylvania State University

Submitted in partial fulfillment of the
requirements for the degree of

MASTER OF SCIENCE IN ELECTRICAL ENGINEERING

from the
NAVAL POSTGRADUATE SCHOOL
December 1971

ABSTRACT

The efficiency of the thermionic diode direct energy converter is dependent upon the interrelated collector temperature, emitter temperature, space charge control and operating load. For instructional purposes it is desirable to be able to vary one parameter at a time while holding the remaining parameters constant. A control system to maintain the collector temperature independent of the other parameter variations is proposed. Using feedback control techniques, a positioning servo mechanism is employed to regulate heat input to the thermionic diode collector. Operating characteristics of the diode and control system results are presented.

TABLE OF CONTENTS

I.	INTRODUCTION	-----	9
II.	OPERATING PRINCIPLES	-----	10
	A. BASIC DIODE OPERATION	-----	10
	B. SPACE CHARGE CONTROL	-----	11
	C. THERMODYNAMIC CONSIDERATIONS	-----	13
III.	DESCRIPTION OF APPARATUS	-----	16
	A. THERMIONIC DIODE	-----	16
	B. VACUUM SYSTEM	-----	21
	C. EMITTER HEAT SOURCE	-----	21
	D. MEASUREMENT DEVICES	-----	21
IV.	THERMIONIC DIODE OPERATING CHARACTERISTICS	----	23
	A. PURPOSE	-----	23
	B. METHODS	-----	23
V.	CONTROL SYSTEM PRINCIPLES	-----	29
	A. CONTROL STRATEGY	-----	29
	B. OPERATIONAL AMPLIFIERS	-----	30
VI.	CONTROL SYSTEM IMPLEMENTATION	-----	33
	A. POSITIONING MECHANISM	-----	33
	B. POSITION ERROR DETECTOR	-----	37
	C. REFERENCE SIGNAL	-----	39
	D. EMITTER TEMPERATURE EFFECTS	-----	39
	E. COLLECTOR TEMPERATURE VARIATIONS	-----	41
VII.	COMPONENT TESTS	-----	46
	A. COLLECTOR THERMAL RESPONSE	-----	46

B.	COLLECTOR TEMPERATURE SIGNAL	-----	49
C.	CLOSED LOOP POSITIONING SYSTEM	-----	52
D.	COLLECTOR TEMPERATURE ERROR	-----	55
VIII.	SYSTEM RESULTS	-----	56
IX.	CONCLUSIONS	-----	59
	BIBLIOGRAPHY	-----	60
	INITIAL DISTRIBUTION LIST	-----	61
	FORM DD 1473	-----	62

LIST OF TABLES

Table

I. Electrode Data	-----	19
II. Operational Amplifier Characteristics	-----	38
III. Collector Response to Step Input	-----	46

LIST OF FIGURES

Figure

1.	Thermionic Diode Electron Potential -----	12
2.	Thermionic Diode Cross-Section -----	17
3.	Cross-Section of Electrode Gap -----	18
4.	Output Voltage Versus Cesium Reservoir Temperature -----	24
5.	Output Voltage Versus Collector Temperature ---	25
6.	Output Voltage Versus Emitter Temperature -----	26
7.	Volt-Ampere Characteristics -----	27
8.	Operational Amplifier as Differential Amplifier--	31
9.	Block Diagram of Basic Positioning System -----	35
10.	Component Diagram of Positioning System -----	36
11.	Heater Voltage Versus Collector Temperature ---	40
12.	Block Diagram of Total Control System -----	42
13.	(a) Component Diagram of Control System -----	43
	(b) Component Identification -----	44
14.	Collector Response to Step Input -----	45
15.	Collector Temperature Signal Differential Amplifier -----	50
16.	Positioning System Closed Loop Response -----	54

LIST OF SYMBOLS AND ABBREVIATIONS

α	Motor mechanical time constant
β	Collector thermal time constant
δ	Retarding potential, volts
η	Efficiency
θ	Angular displacement, radians
μ	Micro
ρ	Density, mass per unit volume
τ	Time, seconds
ϕ	Work function, volts
ψ	Surface potential, volts
ω	Frequency, radians per second
A	Emission constant (area in heat transfer equations)
$^{\circ}\text{C}$	Degrees Centigrade
C	Heat Capacitance
c	Specific heat
E	Error signal
e	Signal potential
EB	Electron bombardment
ev	electron volts
F	Farads
G	Transfer function
h	Heat transfer coefficient
I	Current
J	Current density

$^{\circ}\text{K}$	Degrees Kelvin
K	Gain constant
mm	millimeters
mv	millivolts
q	Heat energy
R	Resistance
s	Time derivative operator
T	Temperature
V	Potential (volume in heat transfer equations)

SUBSCRIPTS

a	Adsorption
C,c	Collector
cd	Conduction
CL	Closed loop
cm	Common mode
E,e	Emitter
fg	Latent heat of vaporization
i	Ionization
j	Joule
o	output
R	Reservoir
ra	Radiation
REF	Reference
s	source
t	thermal (tachometer with gains)
∞	ambient

I. INTRODUCTION

Two thermionic diodes built by Thermo Electron Corporation have been installed in the direct energy conversion laboratory. The purpose of these diodes is to demonstrate the principles of thermionic diode converter operation and the efficiency dependence on the system parameters, in particular, the emitter temperature, collector temperature and space charge control. Each of these parameters is dependent upon the others to varying extents. The operating characteristics of one of the installed diode converters were measured and reported in Ref. 1. The development, theory and principles of thermionic diode converters are presented in detail in Refs. 2 and 3.

This paper will present an overview of the principles of operation as they affect the stabilization of the diode collector temperature during the variation of the other system parameters. Several operating characteristics of the second diode are compared with those reported in Ref. 1. A method for stabilizing the thermionic diode collector temperature is then discussed.

II. OPERATING PRINCIPLES

A. BASIC DIODE OPERATION

The simplest form of the thermionic diode energy converter consists of two electrode surfaces separated by a vacuum or plasma. The emitter surface is maintained at a high temperature. The collector is maintained at a lower temperature. Each electrode surface generates a thermionic current in accordance with the Richardson-Dushman equation [4].

$$J = A T^2 e^{(-\phi/kT)}$$

The constant, A , is the emission constant which is dependent upon the material [4]. The k is Boltzman's constant and T is the absolute temperature of the emitting surface in degrees Kelvin. The ϕ is the work function of the material, that is, the difference in potential between an electron at the surface of the material and an electron removed from the emitting surface to an effectively infinite distance.

With a perfect vacuum between the two thermionic diode electrode surfaces, the energy levels obtained by the thermally generated current electrons in the gap will be the same, that is, the inner electrode gap energy level. This energy level is the sum of the Fermi level of the generating surface plus the surface work function [2, 3, 4]. Therefore, if the emitter material is chosen so as to have a low Fermi energy level and the collector is chosen to have a higher Fermi

energy level, then the electrons in the current generated by the emitter electrode surface arrive at the collector electrode surface with more energy than the electrons remaining on the emitter electrode surface. It is this energy, the difference between the emitter material and collector material Fermi energy levels, that is theoretically available for delivery to an external load. The collector and emitter electrode surfaces of the installed diodes have been cesiated which reduces their work functions significantly as shown in Table I. For this ideal thermionic diode the energy deliverable to the load would be given by:

$$\omega = (\phi_e - \phi_c)(J_e - J_c)$$

B. SPACE CHARGE

In the ideal diode all of the electrons in the thermally generated current had sufficient energy to transit the inner electrode space. And these transits occurred without collisions between the electrons of the opposing currents. In the more realistic model of the thermionic diode the amount of kinetic energy imparted to the electrons above the work function plus Fermi level energy varies and collisions do occur between those generated. A cloud of these low kinetic energy electrons forms in the inner electrode space forming a space charge. This space charge forms an added potential barrier to the currents generated at the electrode surfaces. The energy levels achieved, voltages and electron current flows are shown in Figure 1.

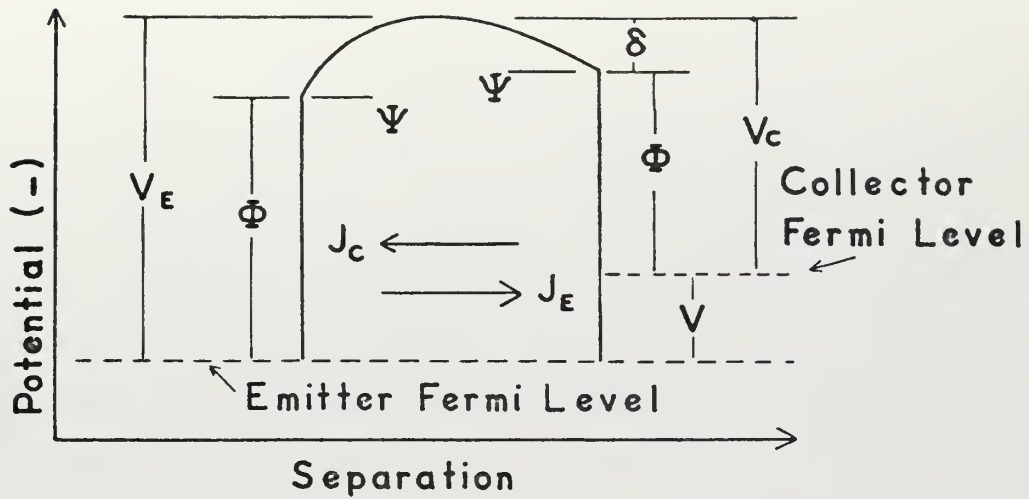


Figure 1. Thermionic Diode Electron Potential

By the formation of this potential barrier and the subsequent loss of current crossing the inner electrode space relative to the currents generated at the surfaces of the emitter and collector, the efficiency of the thermionic diode is greatly reduced. For efficient operation the space charge must be reduced. At present, only one method of space charge control is in use [2]. This method is the introduction of an ionized gas into the inner electrode space to cause recombination with the electrons of the space charge. Cesium is the most commonly used gas material for this purpose. The introduction of the ionized gas causes different potential distributions within the space charge. The various distributions depend on such factors as surface ionization, electron scattering and surface adsorption. These factors produce three principle modes of operation in the cesium controlled space charge implementation of the thermionic diode as an energy converter.

1. Low Pressure Mode

In the low pressure mode the emitter is kept at a sufficiently high temperature to prevent significant surface absorption of the cesium. The inner electrode spacing is kept small enough so that there are few collisions between electrons in the gap. Thus low pressure cesium (10^{-4} mm Hg) provides sufficient ions for neutralization of the space charge electrons.

2. High Pressure Mode

The cesium pressure is high enough (1-10 mm Hg) to cause significant cesium surface adsorption on the emitter surface. The inner electrode spacing in this mode is larger than the mean free path of the generated electrons, thus allowing for the development of the space charge. The degree of space charge control effected by the cesium ions is dependent upon the ionization mechanism in operation. At lower temperatures the ionization of the cesium is by surface ionization; at higher temperatures volume ionization becomes the significant mechanism.

3. Ball-of-Fire Mode

A negative arc drop in an externally heated hot cathode arc (ball-of-fire) is maintained for the purpose of generating the positive ions required for neutralization. The negative space charge is neutralized in the surrounding plasma.

C. THERMODYNAMIC CONSIDERATIONS

In the idealized case the thermionic diode emitter and collector are thermally isolated. Heat is applied to each of

the electrodes to cause the generation of thermionic currents. The difference in energy levels is dissipated as I^2R in the load and leads.

An application of the First Law of Thermodynamics to the emitter electrode and that portion of the inner electrode containing the maximum gap potential requires that

$$\text{ENERGY OUT} = \text{ENERGY IN}$$

$$q_e + q_{fg} + q_{cd} + q_{ra} + q_i = q_c + q_j + q_s + q_a$$

Where q_e is the cooling of the emitter region due to the energy carried away by the emitted electrons. This energy term is proportional to the product of the emitter current density and the potential drop from the maximum gap potential to the emitter Fermi level. The work function energy, or thermodynamically, the latent heat of electron vaporization is represented by q_{fg} . Conduction of heat by the supporting mechanical structure and the attached leads is denoted by q_{cd} . Two categories of heat lost by radiation are encountered. The first loss is heat radiated to the collector electrode. This energy is not only lost to the total energy conversion system but also helps sustain counterproductive J_c . The second category is that radiation that does not strike the collector surface or is not totally reflected to the system by some other surface. This radiant energy is lost to the system. The total radiation energy loss of the emitter is denoted q_{ra} . The last term, q_i , is the heat lost in cesium surface and volume ionization.

Balancing these energy losses to the emitter must be the heat gains. The major heat gain is by the application of heat from an external source, q_s , which is the energy supply to the thermionic diode energy converter and load system. Cesium surface adsorption returns heat as q_a . The energy supplied to the emitter electrode from the collector, q_c , is of the same nature as the q_e loss term, that is, the energy of the thermionic emission current from the collector to the emitter surface. Half of the heating in the lead wires by the Joule effect is attributed to each of the diode electrodes, that to the emitter being q_j . The thermal efficiency of the system would then be calculated as

$$\eta_t = V(J_e - J_c)/q_s$$

where η_t is the thermal efficiency.

III. DESCRIPTION OF APPARATUS

A. THERMIONIC DIODE

The thermionic diodes installed in the energy conversion laboratory are high pressure cesium diodes [1]. A cross-sectional view of the thermionic diode is shown in Figure 2. A view of the diode and gap is shown in Figure 3. Electrode and plasma data are given in Table I. Not shown in Figures 2 or 3 is the emitter electrode heating mechanism, a wolfram, 0.030 inch-diameter heater filament located approximately 0.090 inches above and centered over the emitter electrode assembly. Of particular significance to the problem of thermally stabilizing the diode collector temperature are:

- (1) the emitter-collector inner electrode spacing and the spacing mechanism;
- (2) the location of the collector electrode heater coil and the electrode cooling coil; and
- (3) the thermal mass of the total thermionic diode, cesium heater and associated leads (measured as 767 grams excluding leads and thermocouple assemblies).

In the previous section the collector electrode assembly was considered as a heat sink of the thermionic diode. In the physical realization a heat source and a heat sink are juxtaposed with the collector electrode body assembly. Cooling water is passed through a single loop located below the base plate at a nominal rate of 0.5 gallons per minute. No noticeable effects were encountered if the cooling water flow rate was maintained within twenty percent of the nominal value.

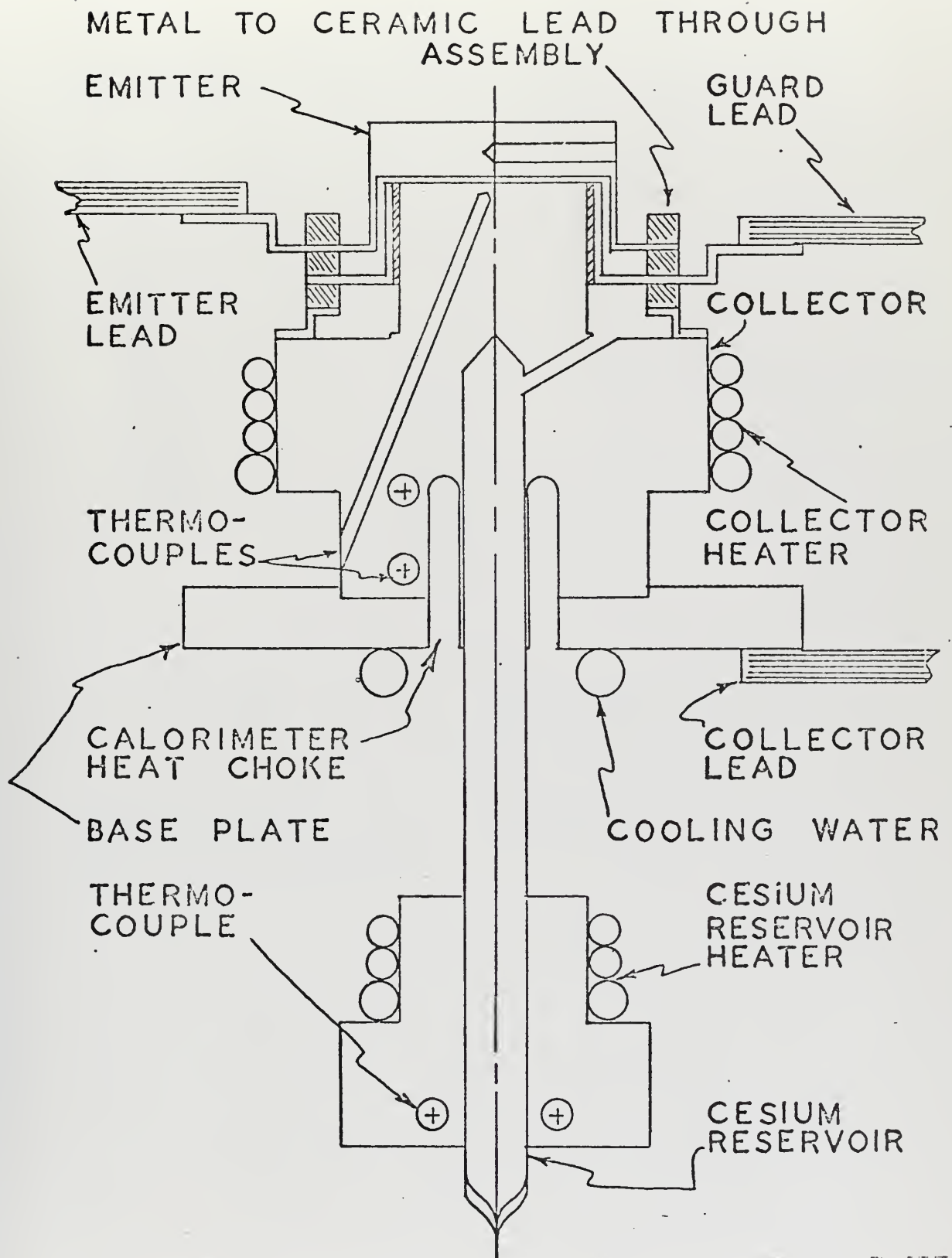


Figure 2. Thermionic Diode Cross-Section (not drawn to scale), Reference 5.

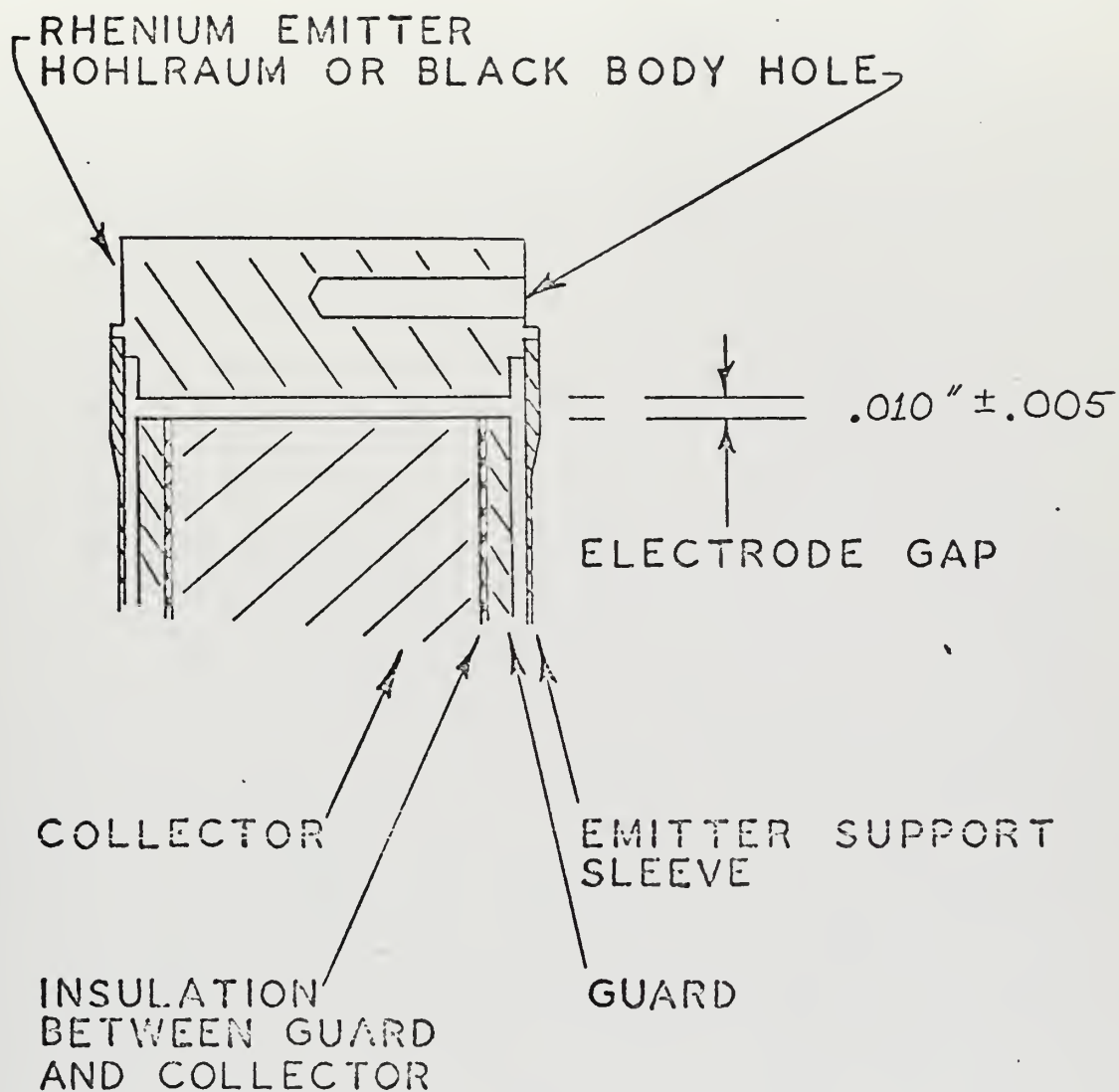


Figure 3. Cross-Section of Electrode Gap (not drawn to scale), Reference 5.

TABLE I
ELECTRODE DATA

	EMITTER	COLLECTOR	PLASMA
MATERIAL [5]	Rhenium (Re)	Niobium (Nb)	Cesium (Cs)
WORK FUNCTION [1]	5.0 electron volts (ev)	3.99 ev	1.81 ev
CESIATED SURFACE [1]	1.98 ev °	1.02 ev	
RICHARDSON'S CONSTANT [1]	266.1	0.05	
ELECTRODE SURFACE AREA [1]	1.833 cm ²	1.533 cm ²	
THERMAL CONDUCTIVITY [10]	20 BTU/hr ft °F	30.5 BTU/hr ft °F	

With the high flow rate cooling water inlet and outlet temperatures varied little. Periodic fluctuations in the inlet source temperature showed no noticeable effects on the collector body temperature. The contribution of the coolant system is to provide a thermal reference base and heat sink to the thermionic diode energy converter.

Due to conduction and radiation losses in the collector and emitter leads, the cesium reservoir and thermocouple leads, heat must be supplied to the collector electrode body by a separate heater system. The collector thermal stabilization method proposed by this paper utilizes this collector heater to accomplish the desired stabilization.

A separate heat source is also provided to heat the cesium utilized for space charge control. By applying heat to the cesium reservoir located below the diode the vapor pressure of the cesium in the diode inner electrode gap is increased. Thus more cesium is available in the gap for space charge control.

The inner electrode gap of the thermionic diode and the connection with the cesium reservoir are maintained at a vacuum of 10^{-8} torr by physical sealing of the diode with a metal-to-ceramic-lead-through assembly [1].

The entire thermionic diode structure of Figure 2 and the emitter electrode heater filament are enclosed in a bell jar to provide for reducing the atmosphere about them. This is done to eliminate heat convection currents and to protect the emitter electrode and heater filament surfaces during high temperature operation.

B. VACUUM SYSTEM

The vacuum system installed is designed to evacuate the bell jar to a pressure of the order of 10^{-6} mm Hg. This is accomplished in two stages by the system provided by Consolidated Vacuum Corporation. The first stage evacuation is by means of a mechanical roughing pump which reduces the bell jar pressure to about ten microns; the second stage reduction to 10^{-6} mm Hg is accomplished by a diffusion pump system.

C. EMITTER HEAT SOURCE

The heat supply to the thermionic diode emitter is from an electron bombardment unit. The electron bombardment unit provides high velocity electrons from a heated filament. Accelerating voltages of up to 1000 volts and bombardment currents of up to 0.3 amperes are provided by the unit. The electron bombardment unit is equipped with a control servo loop which automatically maintains constant bombardment current. This effectively keeps the emitter temperature constant.

D. MEASUREMENT DEVICES

1. Emitter Temperature

The emitter electrode temperature was measured by an optical pyrometer manufactured by the Leeds and Northrup Company [5]. The 8630 series optical pyrometer employed measures the black body temperature of the emitter electrode by color comparison of the holhraum shown in Figure 3 and a heated filament in the pyrometer optics system. Three scales are

provided: low (up to 815°C), high (to 1750°C) and extra high (to 2450°C). Accuracies for the three scales are $\pm 4^{\circ}\text{C}$, $\pm 8^{\circ}\text{C}$ and $\pm 18^{\circ}\text{C}$ respectively. No means of mechanically monitoring the emitter temperature on a continuous basis was available.

2. Collector and Cesium Temperature

The collector electrode and cesium reservoir temperatures were measured by 0.021 inch diameter, sheathed, grounded-junction Chromel-Alumel thermocouples. Response time for this type and size thermocouple is 0.09. seconds [6]. The thermocouple potentials were measured with Leeds and Northrup 8686 Millivolt Potentiometers. The limits of error for the operating range employed are ± 0.03 percent [7]. However, variations of up to two percent were found between potentiometers using identical inputs. A Honeywell Electronik 194 two Pen Ten-Inch Chart Lab Recorder with an accuracy of about one percent was used to make continuous recordings of temperature levels [8].

The temperature accuracies overall were considered to be about two percent to allow for equipment fluctuations and operator error.

IV. THERMIONIC DIODE OPERATING CHARACTERISTICS

A. PURPOSE

Three open circuit voltage characteristic curves were obtained for the thermionic diode under study and one load test was conducted for the diode. These characteristic curves were obtained to ascertain the effective range of parameter variations and to determine the output voltage characteristics as functions of the directly controllable parameters of emitter electrode temperature, collector electrode temperature and the cesium reservoir temperature affecting the space charge control mechanism. The voltage versus amperage curve was obtained to indicate the operation of the diode when acting under a load.

B. METHODS

Experimental constants employed during the determination of the characteristic curves were chosen to match those used for obtaining the same curves reported for the other thermionic diode installation in Ref. 1.

Each point on the curves of Figures 4, 5 and 6 was taken under steady state conditions. Each parameter was adjusted to maintain the desired experimental constants and to achieve the required operating point. About thirty minutes per point were required for the basic system without controls.

Continuous volt-ampere data for Figure 7 was obtained by employing a slide wire as the load resistance. Steady state

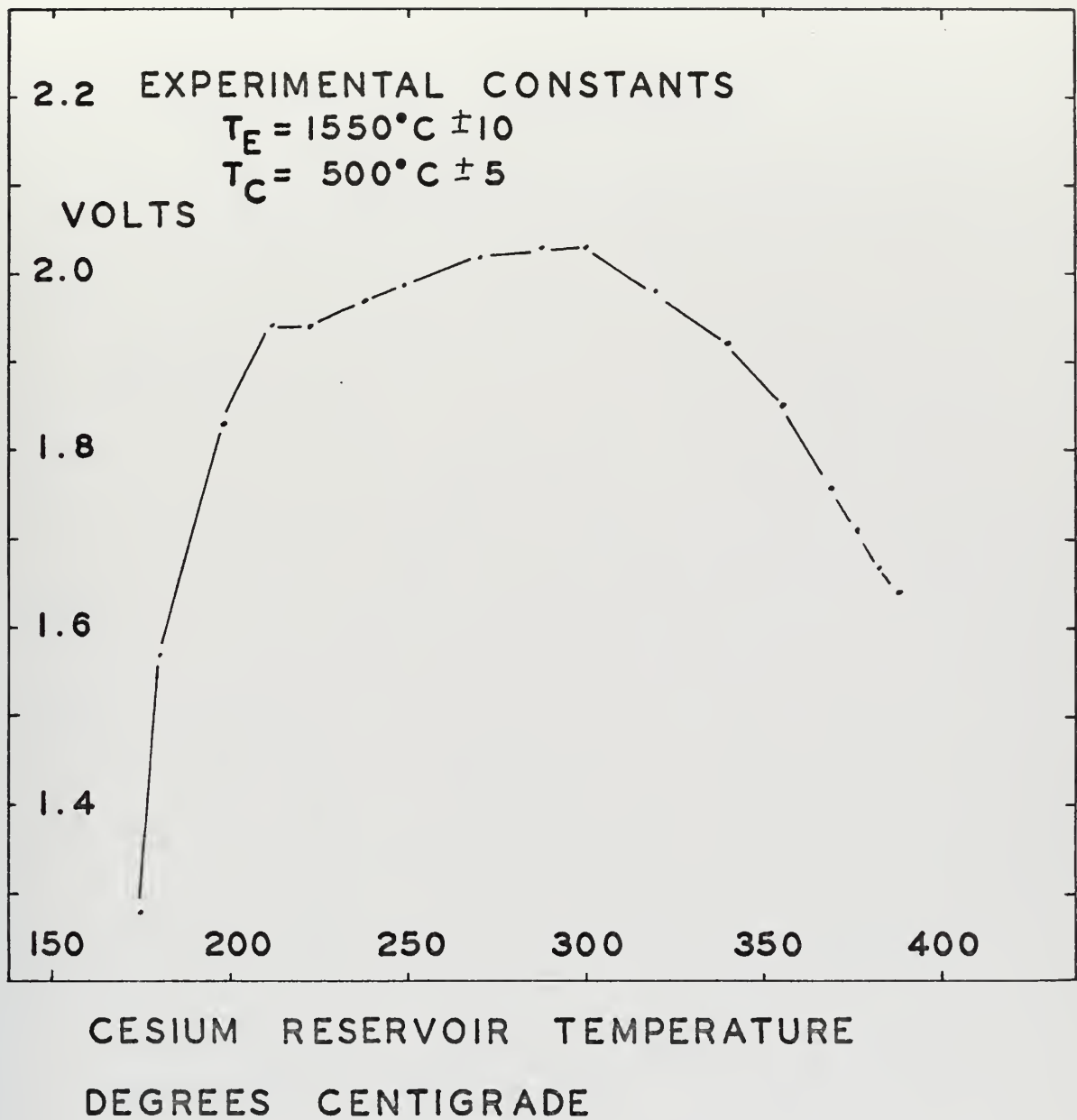


Figure 4. Output Voltage vs. Cesium Reservoir Temperature

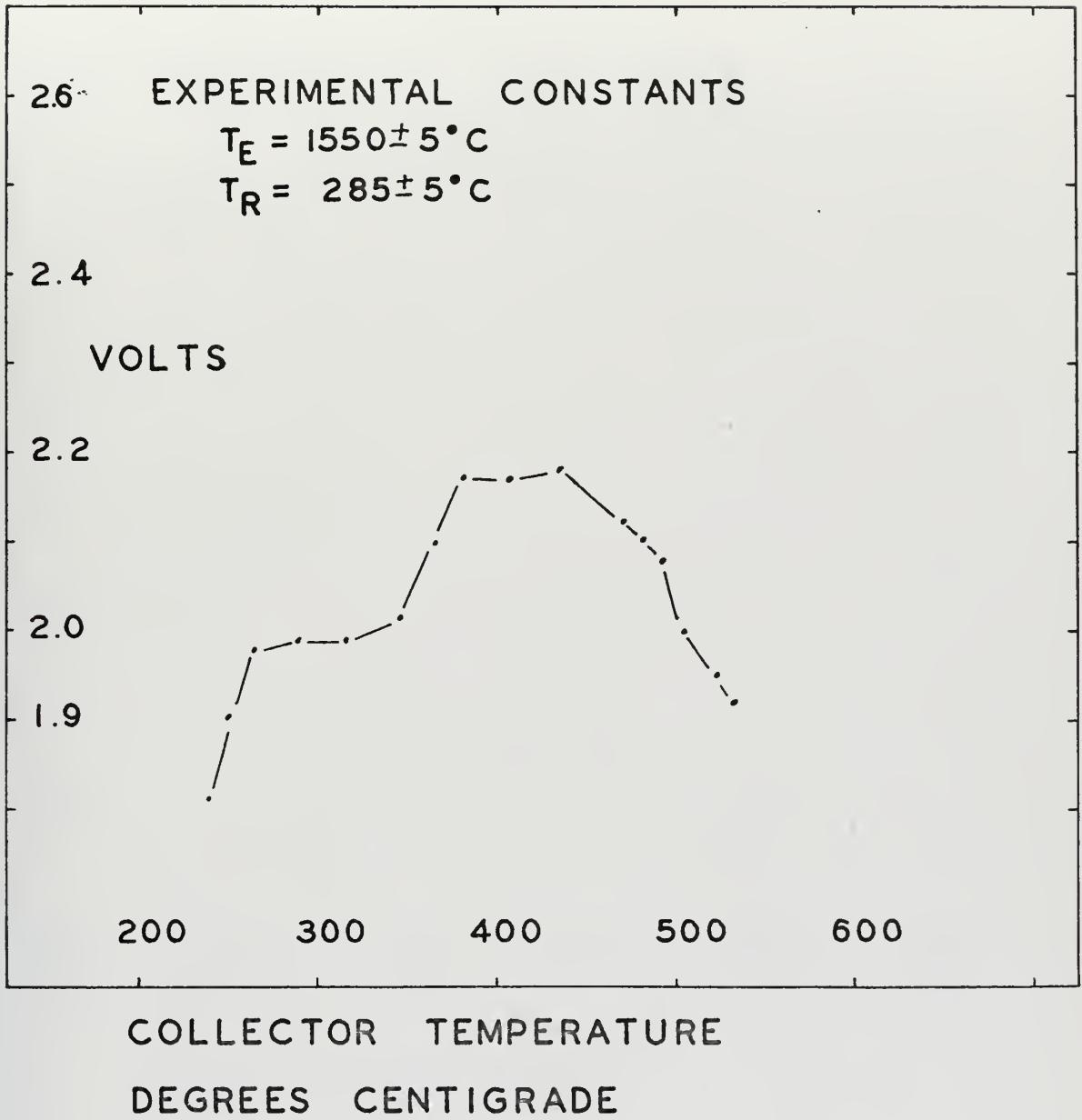


Figure 5. Output Voltage vs. Collector Temperature

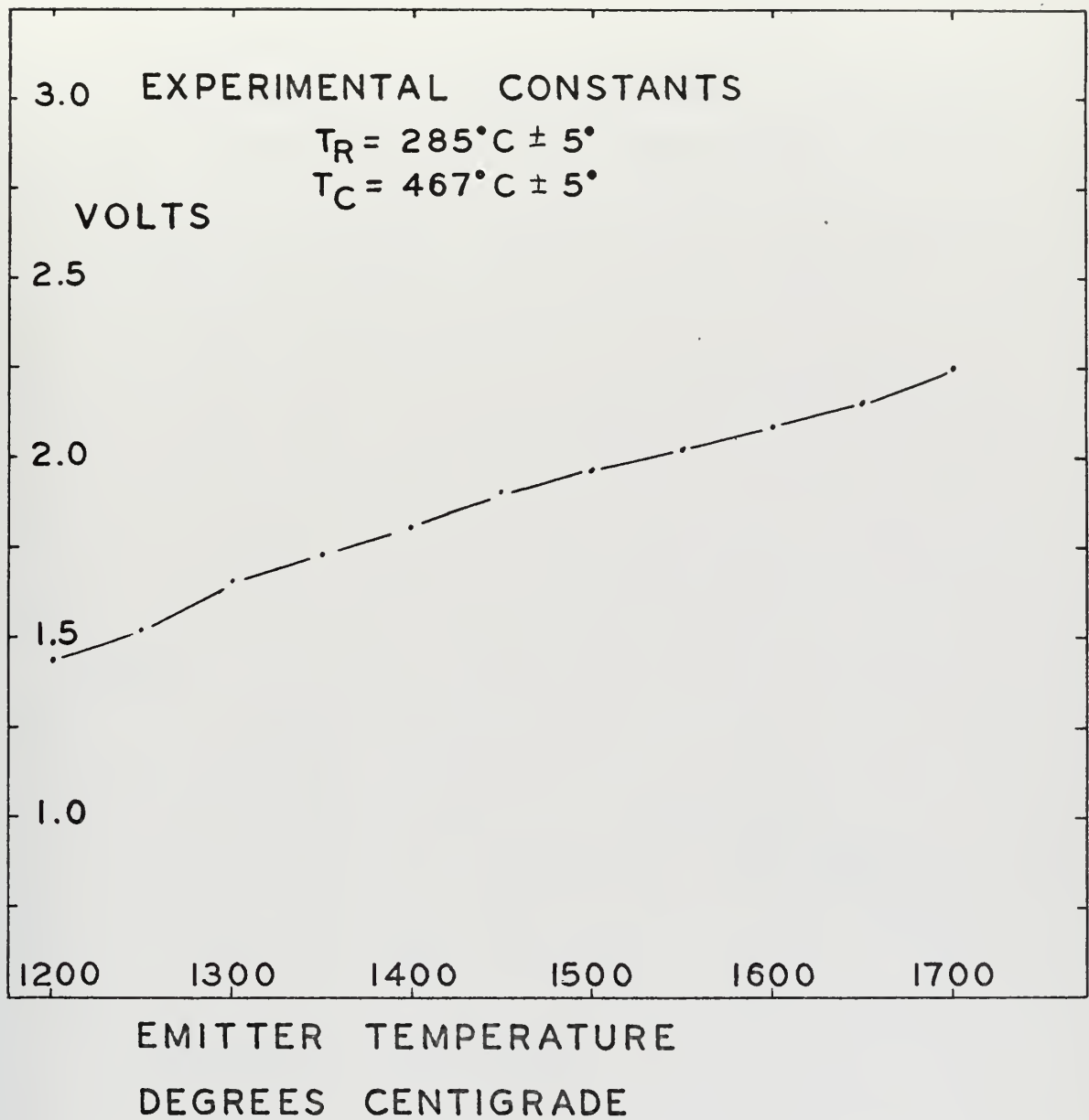


Figure 6. Output Voltage vs. Emitter Temperature

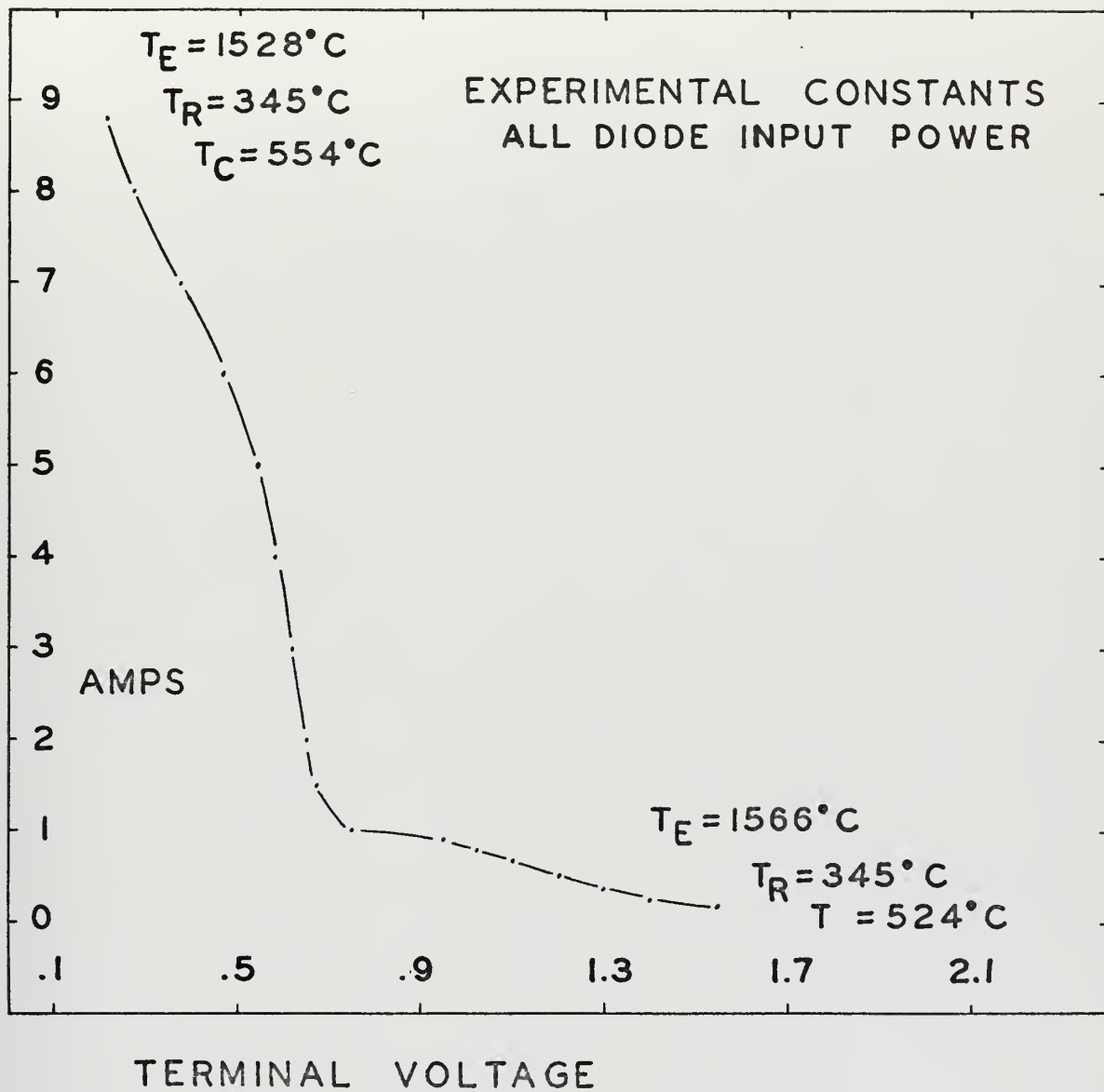


Figure 7. Volt-Ampere Characteristics

conditions were achieved for the initial condition; the slide wire was then moved rapidly in one direction for its entire length with the data being drawn on an X - Y recorder.

The characteristics obtained for this thermionic diode match, in shape and temperature range, the characteristics reported in Ref. 1.

V. CONTROL SYSTEM PRINCIPLES

A. CONTROL STRATEGY

The thermionic diode collector heater is supplied by a 120 volt, 60 hertz single-phase variable transformer with maximum output voltage of 22.5 volts rated at 7.5 amperes. By varying the input power to the heater coil the temperature of the collector may be regulated. The basic control strategy was to measure the diode collector temperature, compare this with a desired reference temperature and then to use the difference signal generated to control the position of the variable transformer.

A DC servo motor and gear train with position and velocity feedback were employed as the positioning mechanism for the variable transformer.

The system plant, in a control theory sense, was considered to be the thermal dynamics of the collector electrode body. Thermodynamically the collector body should respond in accordance with the unsteady state heat transfer equation [9].

$$\frac{T - T_{\infty}}{T - T_0} = e^{-\left(\frac{hA}{\rho CV}\right)\tau}$$

where T is the body temperature in degrees Kelvin; T_{∞} is the ambient or reference temperature and T_0 is the steady state temperature. The time coefficient of the exponential is composed of: h - the heat transfer coefficient; A - the conductive heat transfer cross-sectional area; ρ - the material

density; V - the volume of the body and C the heat capacitance which is the product of V and c , where c is the specific heat of the material. The volume of the body and the conductive heat transfer area can be measured for the collector body; the specific heat and density of the material at various temperatures are available [10]. The heat transfer coefficient is a function of the material, temperature and the configuration of the body [9]. No attempt was made to determine this coefficient due to the complexity of the geometry and multiplicity of temperature levels [11]. Thus no theoretical determination of the thermal time constant was made.

B. OPERATIONAL AMPLIFIERS

The proposed control system employed operational amplifiers for signal gain and signal comparison devices. Operational amplifiers were chosen because of their idealized characteristics of very high input impedance, low drift, low output impedance and favorable noise performance. These characteristics should make them ideal for use with slowly varying millivolt signals.

The differential DC operational amplifier of Figure 8 is governed in the ideal case by the relationship:

$$e_3 = (e_{cm} + e_2) \left(\frac{R_4}{R_3 + R_4} \right)$$

$$\frac{e_{cm} + e_1 - e_3}{R_1} = \frac{e_3 - e_0}{R_2}$$

If these two equations are combined then the output voltage as a function of the input signals is given by

$$e_o = e_{cm} \left[\frac{R_1 R_4 + R_2 R_4 - R_2 R_3 - R_1 R_4}{R_1 (R_3 + R_4)} \right] - \frac{R_2}{R_1} e_1 + \left(\frac{R_4}{R_3} \right) \left(\frac{1 + (R_2/R_1)}{1 + (R_4/R_3)} \right) e_2$$

If the ratio R_2/R_1 is exactly equal to the ratio R_4/R_3 then the output equation reduces to

$$e_o = \frac{R_2}{R_1} (e_2 - e_1)$$

and the common mode signal has been eliminated from the output.

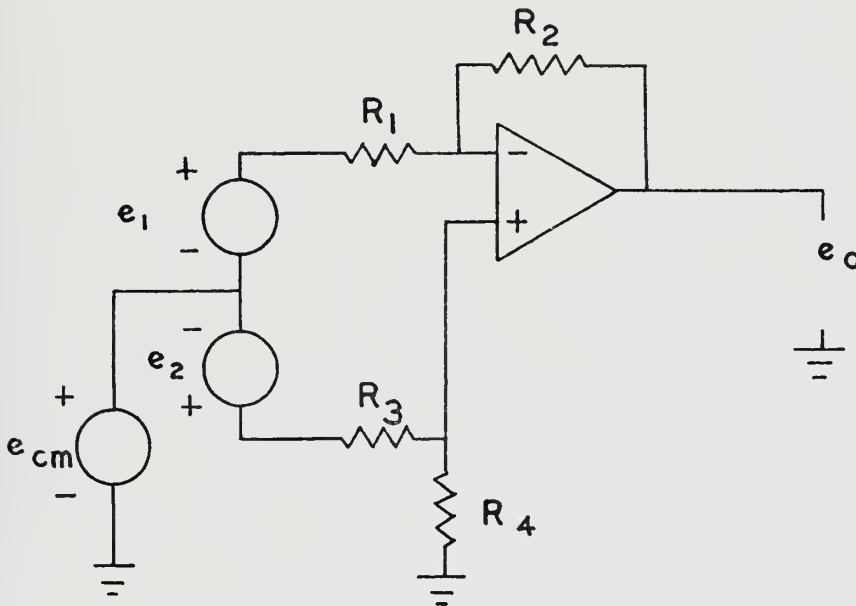


Figure 8. Operational Amplifier as Differential Amplifier

Grounding the positive input terminal through a resistor (R_4) equal to the parallel combination of the input resistor and the feedback resistor produces an inverting amplifier of gain R_2/R_1 . A noninverting amplifier is obtained by grounding the input side of R_1 and applying the input signal to R_4 .

VI. CONTROL SYSTEM IMPLEMENTATION

A. POSITIONING MECHANISM

The heart of the positioning system for the collector temperature controller was an Electro-Craft Corporation DC servo motor with an integral shaft tachometer. The variable transformer provided the mechanical load to the DC servo motor through a gear train and friction coupling.

A DC servo motor and load may be effectively represented by the transfer function

$$\frac{\theta_o}{E} = \frac{K_1}{s(s + \alpha)}$$

where θ_o is the output position, E is the error signal input to the motor, K_1 is the open loop gain constant and α is the mechanical time constant of the motor-load combination [14, 15]. The electrical transient is so short in comparison to the mechanical transient that it can be ignored.

The friction coupling between the servo motor gear train and the variable transformer provided overload protection to the motor when the variable transformer was run into its mechanical stops. Slippage in the coupling was not a contributory factor over the normal range of variable transformer operation. Slippage as could occur was accounted for as saturation in the gain factor of the variable transformer.

The position feedback information for the control system was taken from the variable transformer position. The

voltage supplied to the collector heater coil was rectified in a full wave diode rectifier, filtered to remove the ripple from the signal and then compared with the reference position signal in an error detector. This error detector, as well as most of the other error detectors and amplifiers of the control system, employed a Fairchild $\mu A741C$ operational amplifier configured as a differential amplifier.

A block diagram of the positioning mechanism including position and velocity feedback paths is shown in Figure 9. A drawing of the system component configuration is given in Figure 10. Assuming the control system is operating within the linear limits of the variable transformer then the following set of equations describe the formation of the closed loop transfer function of the position control system:

$$\begin{aligned}
 G_1 &= \frac{K_1/s(s + \alpha)}{1 + \frac{K_1 K_t s}{s(s + \alpha)}} = \frac{K_1}{s(s + \alpha) + K_1 K_t s} \\
 &= \frac{K_1}{s(s + (\alpha + K_1 K_t))} \\
 G_2 &= K_R G_1 \\
 &= \frac{K_1 K_R}{s(s + (\alpha + K_1 K_t))}
 \end{aligned}$$

now forming the closed loop transfer function for the outer loop:

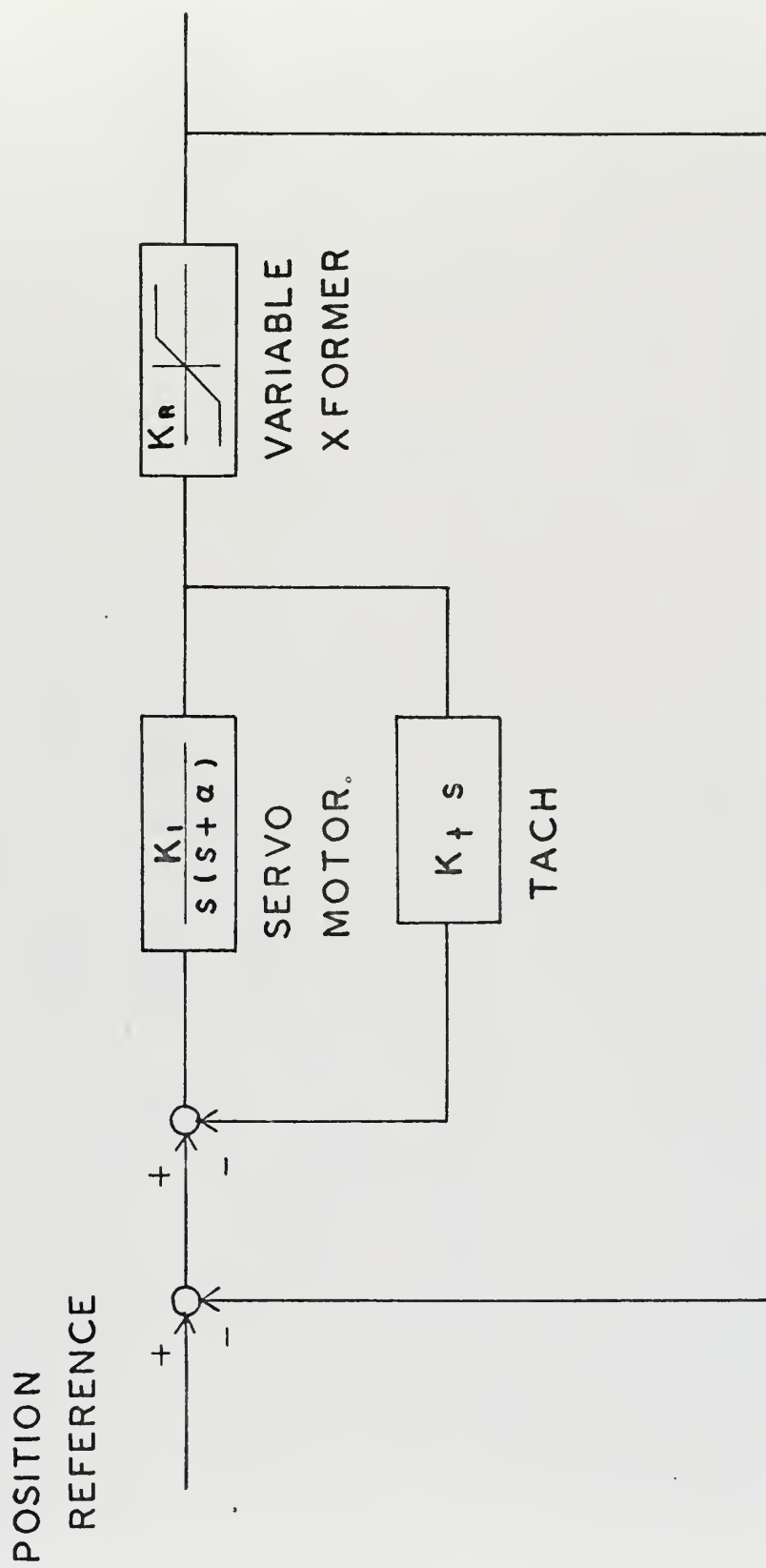


Figure 9. Block Diagram of Basic Positioning System

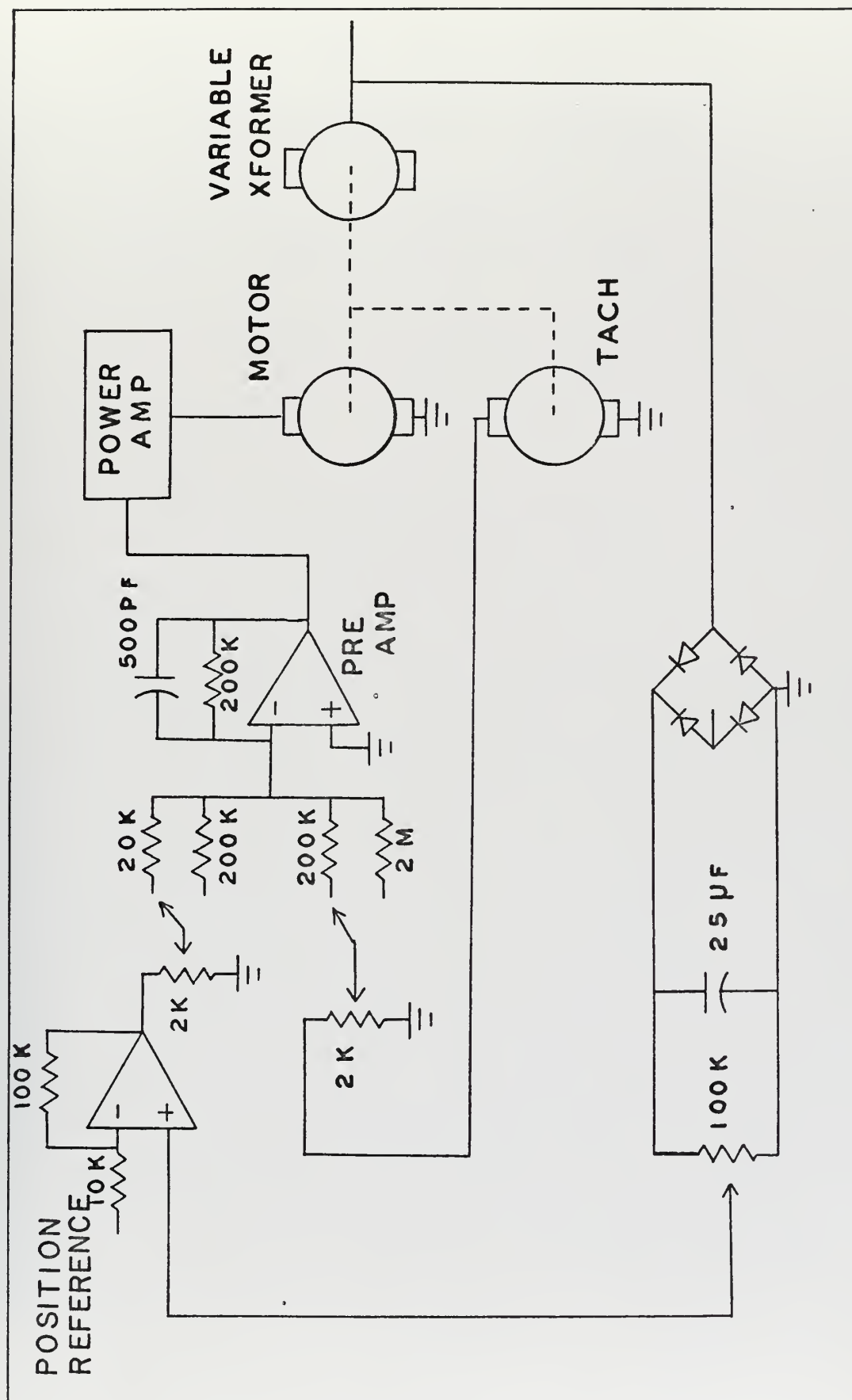


Figure 10. Component Diagram of Positioning System

$$\begin{aligned}
G_{cL} &= \frac{G_2}{1 + G_2 H} \\
&= \frac{K_1 K_R / s(s + (\alpha + K_1 K_t))}{1 + K_1 K_R H / s(s + (\alpha + K_1 K_t))} \\
&= \frac{K_1 K_R}{s(s + (\alpha + K_1 K_t)) + K_1 K_R H} \\
&= \frac{K_1 K_R}{s^2 + (\alpha + K_1 K_t)s + K_1 K_R H}
\end{aligned}$$

which is of the form

$$G = \frac{K}{s^2 + 2\zeta\omega_n s + \omega_n^2}$$

B. POSITION ERROR DETECTOR

The $\mu A741C$ operational amplifier device was chosen as the error detector mechanism. The $\mu A741C$ is a high performance monolithic operational amplifier particularly useful as a voltage follower due to its high common mode range and absence of "latch up" [16]. Electrical characteristics of the 741 operational amplifier are given in Table II. A major factor in the choice of the 741 was its offset null capability. This is the ability to adjust the amplifier online to insure zero output for zero input. The $\mu A741C$ used for the error detector is in the differential amplifier configuration of Figure 8 but with the negative sides of both signals going to ground. This means that there is no common mode signal to the differential amplifier.

TABLE II
OPERATIONAL AMPLIFIER CHARACTERISTICS

Integrated Circuit μ A741C				
Electrical Characteristics (± 15 volts reference, ambient temperature = 25°C)				
<u>Parameter</u>	<u>Minimum</u>	<u>Typical</u>	<u>Maximum</u>	<u>Units</u>
INPUT OFFSET		2.0	6.0	mv (millivolts)
OFFSET VOLTAGE ADJUST RANGE		± 15		mv
INPUT VOLTAGE RANGE		± 15		volts
COMMON MODE REJECTION RATIO	70	90		decibels
INPUT RESISTANCE	.3	2		megohms
OUTPUT RESISTANCE		75		ohms
SLEW RATE		.5		volts/ μ second

C. REFERENCE SIGNAL

The reference position input signal to the error detector was derived from a Leeds and Northrup 8686 Millivolt Potentiometer operating in the EMF Output mode. The potentiometer output was amplified by two operational amplifiers in series. Each amplifier was connected in the inverting mode. Two stages of amplification were employed because an intermediate amplification of the reference signal was desired for use elsewhere in the system.

D. EMITTER TEMPERATURE EFFECTS

If the collector electrode temperature were solely a function of the collector heater input then the control system described in the above sections would suffice. However, the effect of the emitter electrode temperature on the collector temperature is significant. The effect of the emitter temperature on the heater input requirements to obtain a given collector temperature is shown in Figure 11.

The emitter temperature is controlled by a closed loop servo mechanism which controls the electron bombardment current. The bombardment current level servo reference signal is then a direct indication of the emitter temperature. The reference signal is set by adjusting the position of a variable potentiometer which is supplied by a one and a half volt reference battery. By comparing the voltage level on the arm of the potentiometer with a reference level signal and "emitter difference" signal was formed. A μ A741C was again

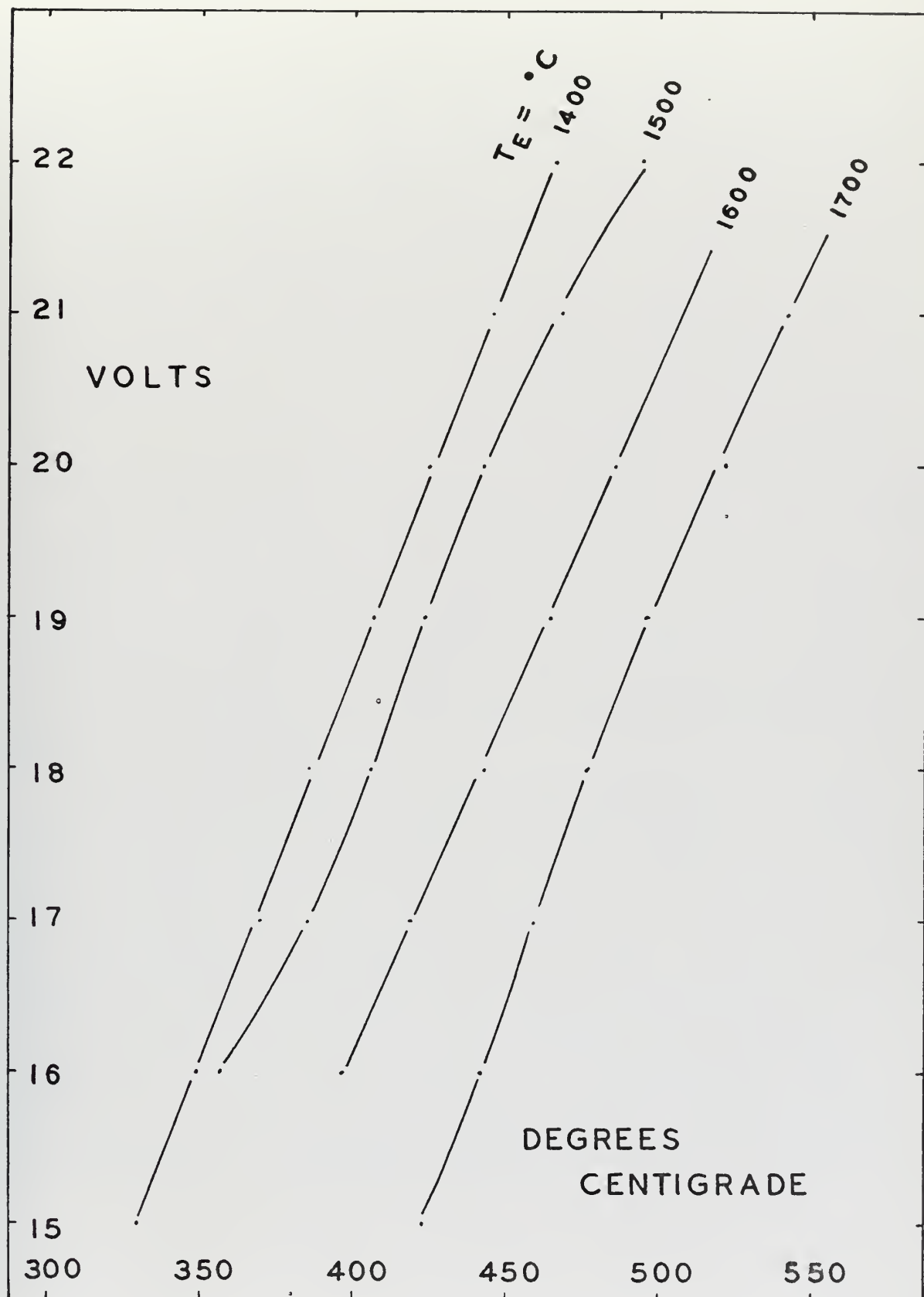


Figure 11. Heater Voltage vs. Collector Temperature

utilized to form the differential amplifier. This emitter difference signal was added to the basic collector temperature reference signal and formed the reference for comparison with the position feedback signal.

E. COLLECTOR TEMPERATURE VARIATIONS

In the scheme above with the modified reference signal there is still no feedback of the output of the plant to the controller input. To close the loop, the measured state of the plant, the collector electrode temperature, must be fed back and compared with the reference signal. The major cause of change in the state of the plant that has not been accounted for so far in the control system is variation in the diode output. The load effect on the collector electrode temperature was nonlinear and highly dependent on the operating point of the diode.

The collector temperature was measured with a Chromel-Alumel thermo couple; the millivolt output of the thermocouple was then amplified in an inverting amplifier and compared with the amplified and inverted reference signal. This collector temperature error signal was then added to the position error signal to form the input signal to the servo motor input amplifier. A block diagram of the complete system is shown in Figure 12 and a component diagram is given in Figure 13.

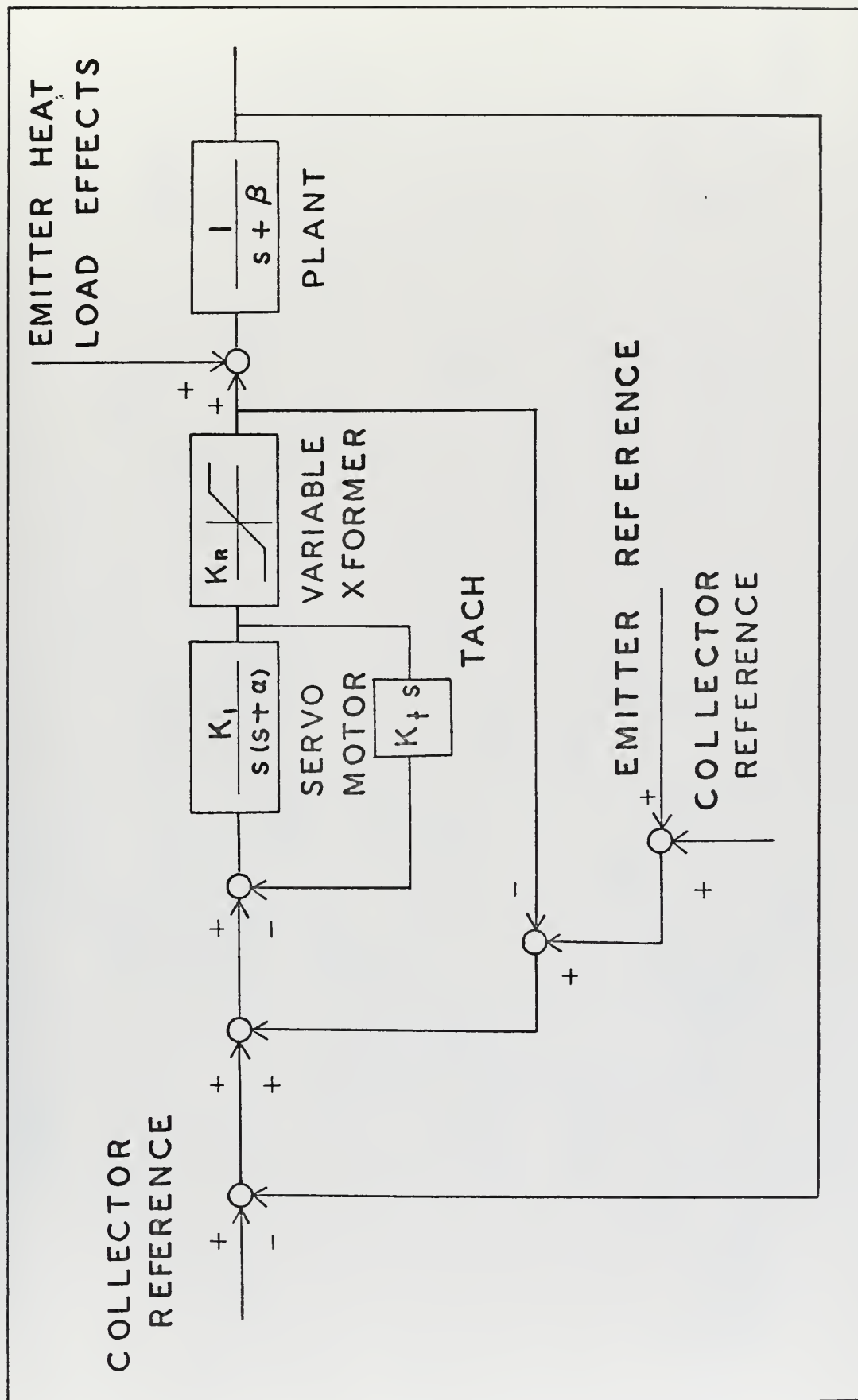


Figure 12. Block Diagram of Total Control System

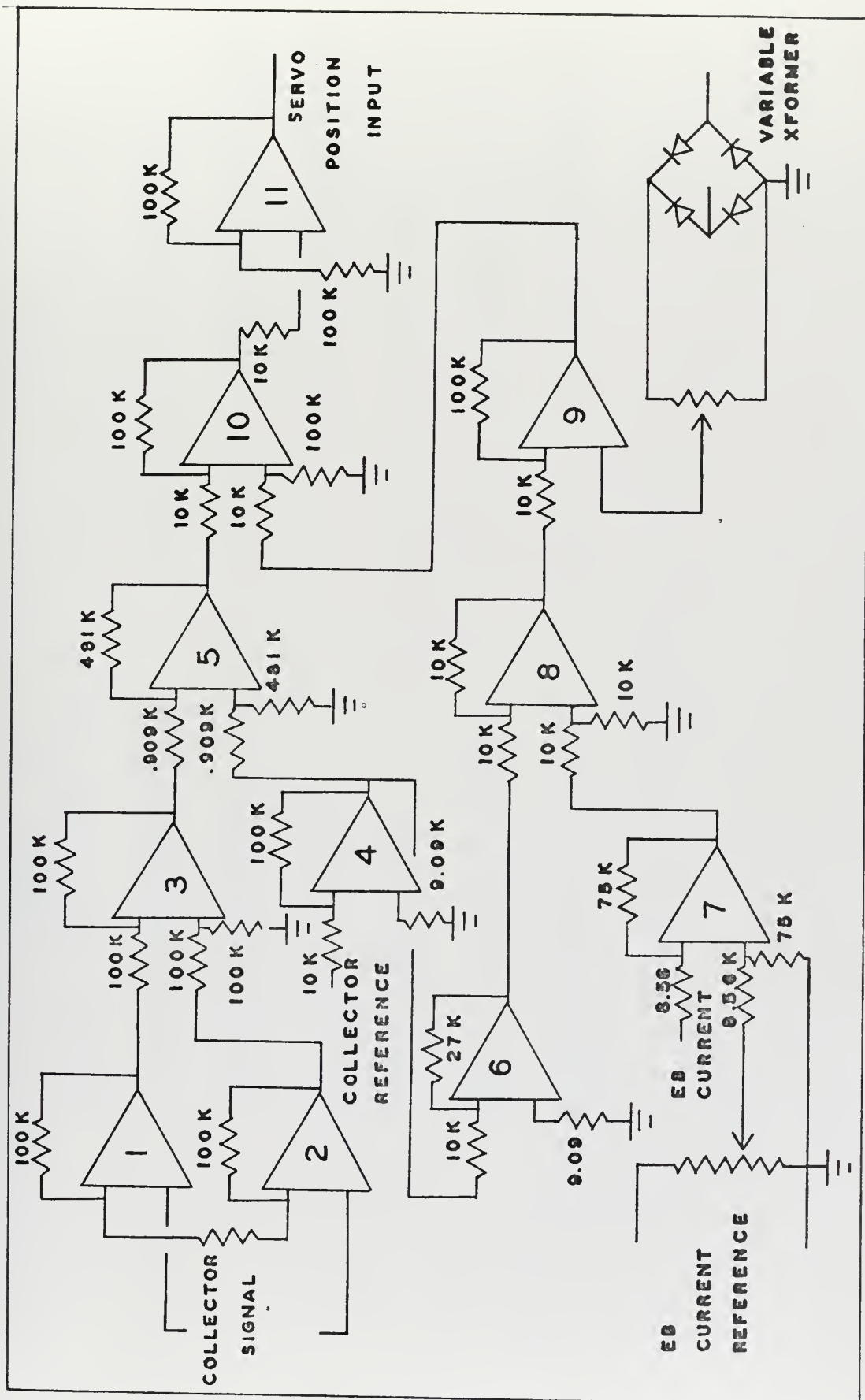


Figure 13a. Component Diagram of Control System

<u>AMPLIFIER</u>	<u>INPUTS</u>	<u>PURPOSE</u>
1,2,3	Collector thermocouple leads	Differential amplifier to obtain temperature signal
4,6	Collector reference signal from source potentiometer	Reference signal amplifiers
5	Collector reference Collector temperature	Collector temperature error detector
7	EB current level signal EB current reference	Emitter temperature difference signal
8	Collector reference Emitter temperature difference	Position reference signal
9	Position reference signal Position feedback signal	Position error detector
10,11	Collector temperature error Position error	Servo position input error signal

Figure 13b. Component Identification

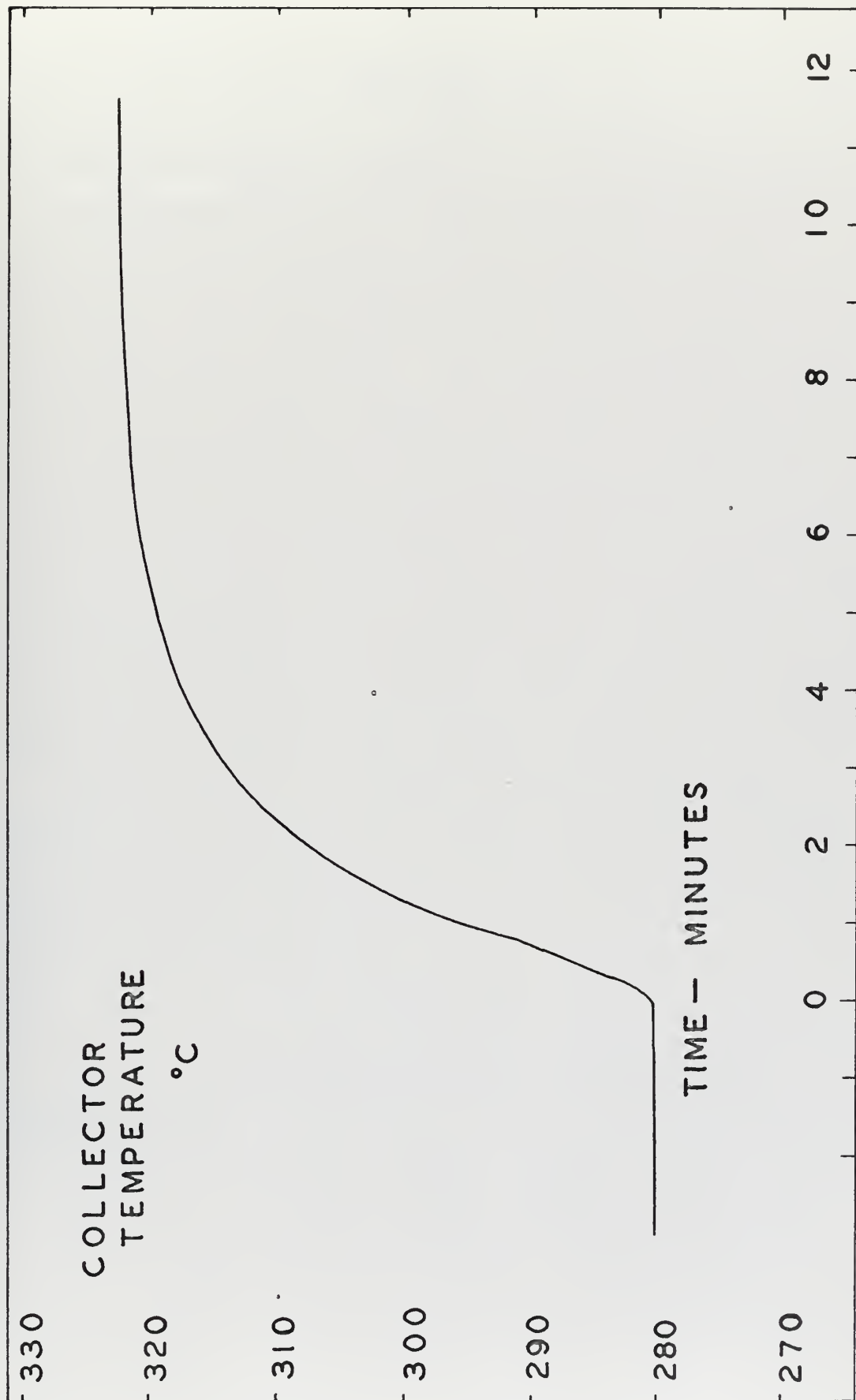


Figure 14. Collector Response to Step Input

VII. COMPONENT TESTS

A. COLLECTOR THERMAL RESPONSE

The response of the collector electrode to a step input in the collector heater power was measured over the range of desired collector temperatures with the emitter and cesium temperatures held constant. Tests were made with emitter temperatures of 1400°C, 1550°C and 1700°C with cesium temperatures of 285°C and 350°C at each emitter temperature. Steps were made both in increasing and decreasing temperature directions. Within the accuracy of the measuring and recording devices the measured thermal response well matched the single time constant exponential response form predicted by the unsteady state conductive heat transfer equation.

Typical results are shown in Figure 14 and Table III. The collector was brought from a steady state temperature of 281°C (11.42 millivolts thermocouple signal) to a final temperature of 322°C (13.15 millivolts).

TABLE III
COLLECTOR RESPONSE TO STEP INPUT

Potential/Time	0	1	2	3	4	5
Predicted	11.42	12.51	12.82	13.02	13.12	13.15
Measured	11.42	12.48	12.88	13.04	13.11	13.15
Input Step = 1.73 mv Time Constant = 1.92 min.						

Calculations were made in the recorded millivolts instead of degrees to preserve the fullest accuracy available. The Chromel-Alumel thermocouple nearest to the collector electrode inner gap surface was used as the effective measurement of the collector electrode temperature; the lower thermocouples were checked to verify steady state conditions.

The collector electrode thermal response was also tested by applying step increases and decreases to the electron bombardment current. Although the heat transfer mode then included radiation and the heat transfer cross-sectional area for this input is different, the response of the collector electrode was effectively the same as for the heater input steps and showed the same time constant as for the heater input.

Cesium reservoir temperature changes showed no noticeable effects on the collector temperature during open circuit tests.

The effects of load resistance variations on the collector temperature were extremely dependent upon the overall operating point, i.e., the combination of the emitter temperature, collector temperature and cesium reservoir temperature. At lower temperatures (T_E below 1600°C and T_C below 500°C with cesium temperature below 330°C) the effects were negligible. At the higher temperatures where volume ionization of the cesium becomes significant the collector temperature varied by as much as fifty degrees in the uncontrolled system. This is the region of operation which initiated consideration of implementing a control system.

(This page intentionally blank)

During the latter part of the experimental period available for testing the system the filament of the electron bombardment unit failed. A replacement filament was manufactured by laboratory personnel from available sources of 0.030 inch tungsten wire. No dimensions of the filament other than the diameter were available and the old filament was destroyed beyond use as a pattern. The manufactured filament did not match the characteristics of the original filament. The maximum emitter electrode temperature obtained with the new filament was 1625°C. Up to fifty percent more bombardment current was required to achieve the same emitter temperature achieved by the original filament. This greatly hampered measurements of the effectiveness of the proposed control system.

B. COLLECTOR TEMPERATURE SIGNAL

Using grounded sheathed thermocouples improves the response time of the thermocouple but it also places the lower potential of the thermocouple at the potential of the material in contact with the sheath. The Alumel side of the collector electrode thermocouple was thus at the collector potential which varies throughout the operating range of the thermionic diode. The Chromel lead of the thermocouple is then at the collector potential plus the potential generated by the thermocouple. When measuring the collector temperature with the Leeds and Northrup 8686 Millivolt Potentiometer or with an ungrounded recorder no difficulty was encountered in obtaining good indications of the collector electrode temperature.

Amplification of the millivolt thermocouple potential riding on the variable collector electrode potential proved difficult. The differential amplifier configuration of Figure 8 failed to block the common mode collector potential signal. Cascading amplifiers to improve the common mode rejection ratio failed to achieve the desired results. A combination of three operational amplifiers as shown in Figure 15 produced acceptable results.

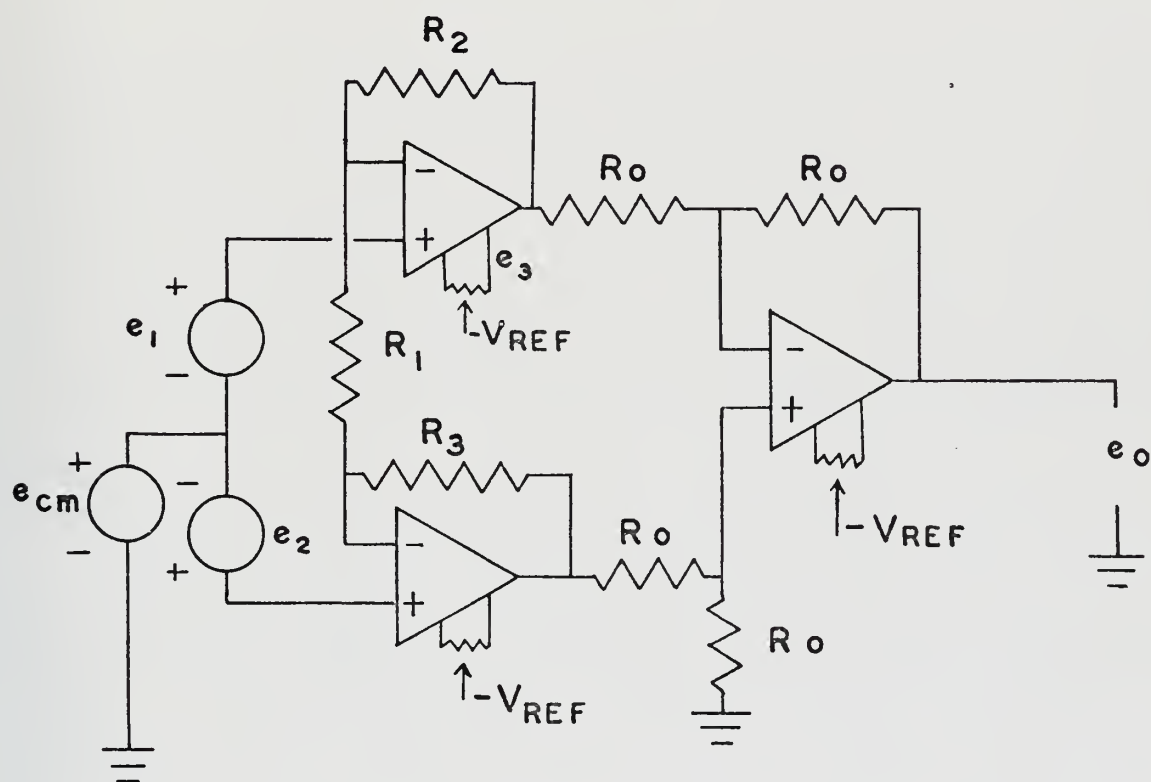


Figure 15. Collector Temperature Signal Differential Amplifier

Analysis of this circuit yields the following equations

$$e_3 = (1 + R_2/R_1)e_1 - \frac{R_2}{R_1} e_2 + e_{cm}$$

$$e_4 = (1 + R_3/R_1) e_2 - \frac{R_3}{R_1} e_1 + e_{cm}$$

$$e_o = e_4 - e_3$$

If $R_2 = R_3$, then the output voltage is

$$e_o = (1 + \frac{2R_2}{R_1}) (e_2 - e_1)$$

A value of 100 k was chosen for R_o and R_2 using one percent precision resistors to effect a good match. The two input amplifiers constitute a differential buffer amplifier with a gain of $(1 + 2 R_2/R_1)$ for the differential signals and unity gain to common mode signals. Mismatch of R_2 and R_3 creates a gain error but does not effect the common mode rejection ratio.

Even with the configuration of operational amplifiers given in Figure 15, problems were encountered with collector potential variation effects on the amplified collector temperature signal. Stepping from open circuit to loaded conditions resulted in signal jumps of up to 0.5 millivolts on the unamplified signal. This represents an indication of a jump in temperature of about ten degrees; it was apparent that this signal change was in the indicating system as a jump of this type could not actually occur in the collector temperature. This amplifier configuration also produced greater noise perturbations on the amplified temperature signal than were encountered with a

single stage or two stage series differential amplifier. The magnitude and frequency of the noise was such that it provided no particular degradation of the control system performance but was of significance only in its blurring effect on the recording of the temperature signal.

To achieve good results the nulling circuits shown on the amplifiers of Figure 15 had to be adjusted before each day's operation. This required shorting the input terminals to each amplifier to insure zero input signal and then adjusting the null circuit potentiometer to achieve zero output. A significant change in the potentiometer setting would be required to accomplish the zeroing. Both buffer amplifiers would be nulled first and then with a common input signal to these two amplifiers the output stage would be nulled. The R_1 resistance was configured as a variable potentiometer to allow correction for observed drifts in the differential amplifier gain.

C. CLOSED LOOP POSITIONING SYSTEM

The positioning system was first tested as a closed loop system by applying a step input to the position reference node. Transient response measurements were made with the tachometer gain set at one, ten, fifty and one hundred. Settling times were taken as the time at which the output reached and maintained a condition of less than five percent variation from the final value. The settling time was the prime consideration in the selection of the gain settings. Percent peak overshoot and time of overshoot were noted but not considered to be of particular significance in this application. Steady

state error was of course considered. The transient response was recorded for position gain settings of one, ten, twenty, and one hundred. The response recorded for potentiometer settings of one hundred for both position and velocity signals is shown in Figure 16. Through second order curves the following factors for the system were derived from Figure 16; a peak to steady state magnitude ratio of 1.12, peak time of 1.55 seconds, settling time of 4.3 seconds, damping factor of 0.48 and frequency of 2.25 radians per second.

The amplifier-servo motor system displayed a dead zone characteristic. An input of ± 0.05 volts was required to the servo position gain potentiometer (with gain set at one hundred) to initiate servo motor motion. With 0.05 millivolts representing a temperature difference of one degree through the thermocouple, a signal gain of at least one thousand was required to insure initiation of position change for a one degree alteration in the desired temperature.

The gear train installed between the servo motor shaft and the shaft of the variable transformer provided a ratio of 80 to 1. Backlash in the gear train combined with 0.07 radians freeplay in the brush position on the arm of the variable transformer necessitated 2.8 radians of motion at the servo motor to take up maximum slack and to start transformer motion.

The accumulative effect of these nonlinearities can be seen as an error in the steady state output position resulting from the step input in Figure 16. No particular ripple on the output was noted during the tests of the positioning loop as a component.

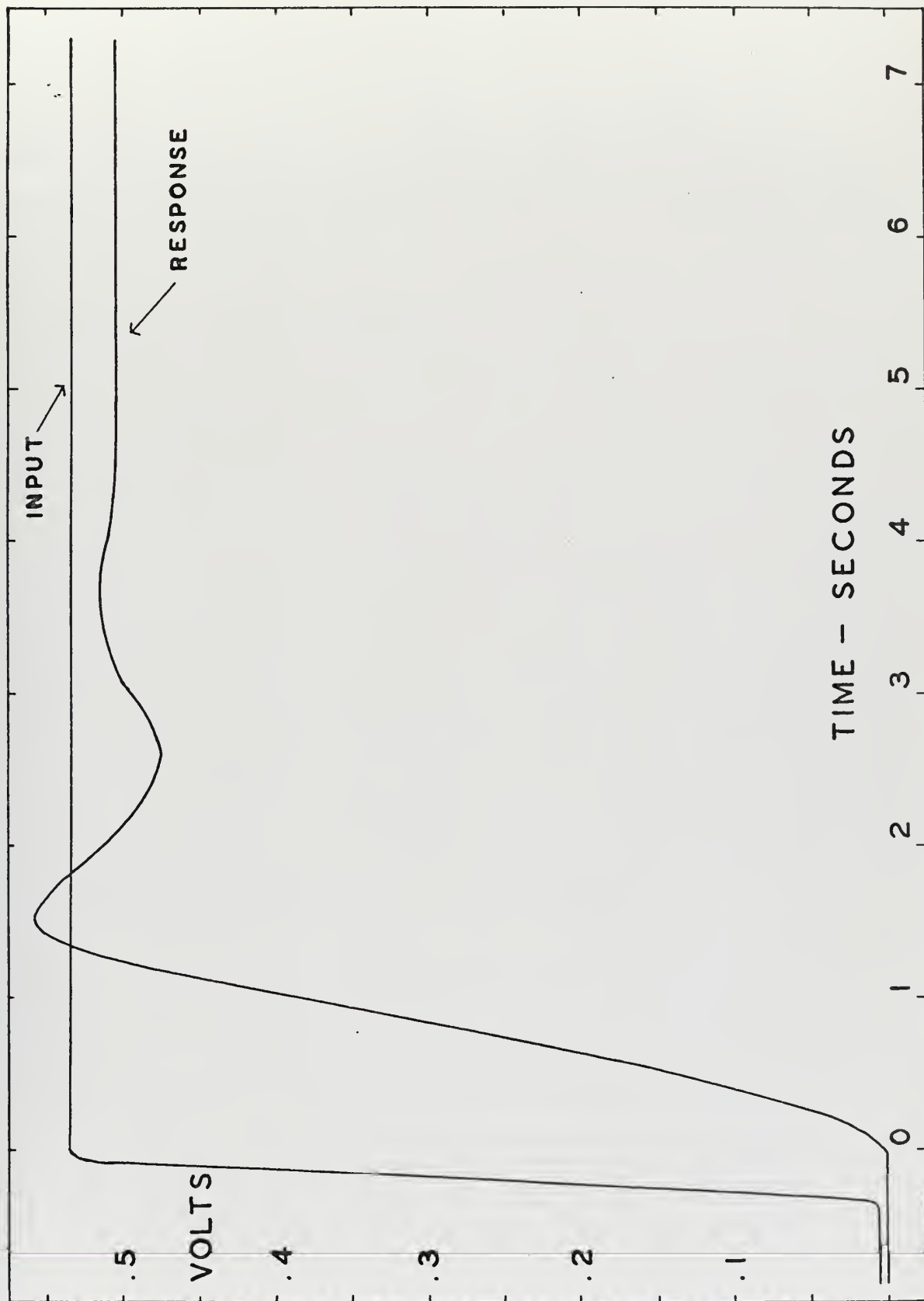


Figure 16. Positioning System Closed Loop Response

The position feedback signal generated through the rectifier system was linear throughout most of its desired operating range with a DC signal to heater AC voltage ratio of 0.085 volts DC per AC volt. Slight upward curvature of the DC versus AC plot was noted both below 10 volts AC and above 22 volts AC.

D. COLLECTOR TEMPERATURE ERROR

As occurred with the collector temperature differential amplifier, drift was encountered in the output voltage of the two signal amplifiers and the error detector differential amplifier. With shorted inputs the null circuits of the two signal gain amplifiers would be set to zero the output. It was found that if the differential amplifier was tested with the shorted inputs to the other amplifiers that noise signals would inhibit proper amplifier nulling. If a common signal greater than about two millivolts was introduced to the signal amplifiers then the null adjustment for the differential amplifier could be achieved with relative ease.

VIII. SYSTEM RESULTS

The total control system was tested at emitter temperatures of 1400°C, 1550°C and 1625°C with low and high cesium temperatures. Various collector temperature settings between 300°C and 525°C were employed. Both open circuit and load tests were conducted under the various operating points.

At lower temperatures the collector temperature was stabilized to within ± 3 degrees of the desired temperature with little drift about the steady state point. Initial settling time for large step changes in temperature (such as at start-up time) were on the order of seven to ten minutes with overshoots on the order of twenty percent. The significant contribution under these conditions is that the student operator is relieved of the guess work as to what heater power setting to employ to obtain the desired temperature. The only action being required would be to set the desired temperature into the reference collector temperature setting. Without the controller it would typically require two or three times the settling time of the plant to observe the collector temperature and attempt to manually adjust the heater power as the desired temperature was approached. Similar improvements were achieved, for the low temperature operating region, in the maintenance of the desired temperature as the emitter temperature, cesium temperature or load were varied. Maximum collector temperature variations of five degrees during transitions were above the two degrees typically encountered.

At higher temperatures, where volume ionization of the cesium becomes effective, stability was achieved but in a more general sense. The collector temperature could be maintained only to within ± 6 degrees. The collector temperature under these conditions would vary in an approximately sinusoidal fashion with periods of from one half to two cycles per minute depending upon the gain setting of the servo motor position potentiometer, increasing in frequency with the higher gain settings. It was under the higher operating conditions that the current delivered by the thermionic diode became significant; the heating effects of the current on the diode electrodes enters directly to the plant and not through the controller. Although the emitter temperature effect enters directly also, compensation was simultaneously introduced to the controller reference.

In combination with the current effects was the accumulative effect of the nonlinearities within the system. The oscillation on the plant output is characteristic of backlash and deadspace.

The positioning system used for this implementation was an off-the-shelf laboratory setup utilized in the servo laboratory by students to study such nonlinear effects as deadspace, backlash and relay controls. An improvement in the system performance could certainly be obtained by improving the gear train to reduce backlash. The brush on the variable transformer could also be stiffened to reduce the lost motion encountered there.

Improvement in the error detector systems might be achieved by employing multiple amplifier single chip integrated circuits which would show identical thermal tracking characteristics for each amplifier. A single temperature compensation circuit might then be employed to restrict the drift demonstrated by the amplifiers in the present arrangement of eleven operational amplifiers with eleven potentiometers.

If the system as implemented were to be used and the dither were found to be excessive then the present controller could be used to achieve the vicinity of the desired temperature and then be shut off to allow manual control in the final stage.

IX. CONCLUSIONS

The thermionic diode energy converter investigated showed good agreement with the operating characteristics reported in Ref. 1. A system to control the collector electrode temperature during changes in the emitter temperature, cesium temperature and operating load was implemented. Acceptable stabilization was achieved over the full range of achieved temperature operations; equipment failure during the latter part of the investigative period prevented testing at high emitter temperature where greatest system efficiency is expected. Nonlinearities in the control system produced collector temperature oscillations during higher temperature operations. Reduction of the backlash in the gear system and deadspace in the collector heater variable transformer would improve the system performance.

BIBLIOGRAPHY

1. McCann, W. R., Parametric Variations of the Thermionic Diode, M.S. thesis, Naval Postgraduate School, 1970.
2. Angrist, S. W., Direct Energy Conversion, Allyn and Bacon, 1965.
3. Sutton, G. W., editor, Direct Energy Conversion, McGraw-Hill, 1966.
4. Soo, S. L., Direct Energy Conversion, Prentice-Hall, 1968.
5. Engineering drawing number 641-1000, Thermo Electron Corporation, Waltham, Massachusetts.
6. Optical Pyrometer Manual, 8630 Series, Leeds and Northrup Company.
7. Ceramo Metal Sheathed Thermocouples, Thermo Electric Company, Incorporated, 1965.
8. Directions for 8686 Millivolt Potentiometer, Leeds and Northrup Company.
9. Manual for Two Pen Ten-Inch Chart Electronik 194 Lab Recorder, Honeywell Incorporated, 1967.
10. Touloukian, Y. S. and Buyco, E. H., Thermophysical Properties of Matter, Volume I, IFI/Plenum, 1970.
11. Holman, J. P., Heat Transfer, McGraw-Hill, 1968.
12. Kelleher, M. D. and Pucci, P. F., Department of Mechanical Engineering, Naval Postgraduate School, conversations with.
13. Shick, L. L., Linear Circuit Applications of Operational Amplifiers, IEEE Spectrum, p. 36-50, April 1971.
14. Thaler, G. J. and Brown, R. G., Analysis and Design of Feedback Control Systems, McGraw-Hill, 1960.
15. Thaler, G. J. and Wilcox, M. L., Electric Machines: Dynamics and Steady State, McGraw-Hill, 1960.

INITIAL DISTRIBUTION LIST

	No. Copies
1. Defense Documentation Center Cameron Station Alexandria, Virginia 22314	2
2. Library, Code 0212 Naval Postgraduate School Monterey, California 93940	2
3. Professor M. L. Wilcox, Code 52 Wx Department of Electrical Engineering Naval Postgraduate School Monterey, California 93940	2
4. Dr. G. J. Thaler, Code 52 Tr Department of Electrical Engineering Naval Postgraduate School Monterey, California 93940	1
5. LT R. E. Schantz 1234 Spruance Road Monterey, California 93940	1

DOCUMENT CONTROL DATA - R & D

(Security classification of title, body of abstract and indexing annotation must be entered when the overall report is classified)

1. ORIGINATING ACTIVITY (Corporate author) Naval Postgraduate School Monterey, California 93940		2a. REPORT SECURITY CLASSIFICATION Unclassified	
		2b. GROUP	
3. REPORT TITLE THERMAL STABILIZATION OF A THERMIONIC DIODE COLLECTOR			
4. DESCRIPTIVE NOTES (Type of report and, inclusive dates) Master's Thesis			
5. AUTHOR(S) (First name, middle initial, last name) Robert Edwin Schantz Lieutenant, United States Navy			
6. REPORT DATE December 1971		7a. TOTAL NO. OF PAGES 63	7b. NO. OF REFS 15
8a. CONTRACT OR GRANT NO.		9a. ORIGINATOR'S REPORT NUMBER(S)	
b. PROJECT NO.			
c.		9b. OTHER REPORT NO(S) (Any other numbers that may be assigned this report)	
d.			
10. DISTRIBUTION STATEMENT Approved for public release; distribution unlimited.			
11. SUPPLEMENTARY NOTES		12. SPONSORING MILITARY ACTIVITY Naval Postgraduate School Monterey, California 93940	
13. ABSTRACT <p>The efficiency of the thermionic diode direct energy converter is dependent upon the interrelated collector temperature, emitter temperature, space charge control and operating load. For instructional purposes it is desirable to be able to vary one parameter at a time while holding the remaining parameters constant. A control system to maintain the collector temperature independent of the other parameter variations is proposed. Using feedback control techniques, a positioning servo mechanism is employed to regulate heat input to the thermionic diode collector. Operating characteristics of the diode and control system results are presented.</p>			

KEY WORDS	LINK A		LINK B		LINK C	
	ROLE	WT	ROLE	WT	ROLE	WT
Thermionic diode						



BRINDERY

Thesis

S248

c.1

Schantz

Thermal stabilization of a thermionic diode collector.

133152

BRINDERY

Thesis

S248

c.1

Schantz

Thermal stabilization of a thermionic diode collector.

133152

thesS248

Thermal stabilization of a thermionic di



3 2768 001 00413 8

DUDLEY KNOX LIBRARY